

## Electronic Supplementary Information (ESI)

### **Nano-sandwiched metal hexacyanoferrate/graphene hybrid thin films for in-plane asymmetric micro-supercapacitors with ultrahigh energy density**

*Yafei He,<sup>‡a</sup> Panpan Zhang,<sup>‡b</sup> Mao Wang,<sup>c</sup> Faxing Wang,<sup>b</sup> Deming Tan,<sup>d</sup> Yang Li,<sup>e</sup>  
Xiaodong Zhuang,<sup>a</sup> Fan Zhang,<sup>\*a</sup> Xinliang Feng<sup>b</sup>*

<sup>a</sup> School of Chemistry and Chemical Engineering, Shanghai Jiao Tong University, Shanghai 200240, China, E-mail: fan-zhang@sjtu.edu.cn

<sup>b</sup> Department of Chemistry and Food Chemistry & Center for Advancing Electronics Dresden (cfaed), Technische Universität Dresden, Dresden 01062, Germany

<sup>c</sup> Helmholtz-Zentrum Dresden-Rossendorf, Institute of Ion Beam Physics and Materials Research, Bautzner, Landstr. 400, Dresden 01328, Germany

<sup>d</sup> Department of Chemistry and Food Chemistry, Technische Universität Dresden, Dresden 01069, Germany

<sup>e</sup> Material Systems for Nanoelectronics, Chemnitz University of Technology, Reichenhainer Str. 70, Chemnitz 09107, Germany

<sup>‡</sup> These authors contributed equally to this work.

## **Experimental section**

### **Chemicals and materials:**

All the reagents and solvents, such as graphite flakes, sodium nitrate ( $\text{NaNO}_3$ ), sulfuric acid ( $\text{H}_2\text{SO}_4$ ), potassium permanganate ( $\text{KMnO}_4$ ), copper chloride dihydrate ( $\text{CuCl}_2 \cdot 2\text{H}_2\text{O}$ ), nickel chloride hexahydrate ( $\text{NiCl}_2 \cdot 6\text{H}_2\text{O}$ ), cobalt chloride hexahydrate ( $\text{CoCl}_2 \cdot 6\text{H}_2\text{O}$ ), ferrous chloride tetrahydrate ( $\text{FeCl}_2 \cdot 4\text{H}_2\text{O}$ ), potassium hexacyanoferrate ( $\text{K}_3\text{Fe}(\text{CN})_6$ ), and dimethylformamide (DMF, GC, 99.9%), were purchased from commercial suppliers such as Sigma-Aldrich, Macklin, and Adamas-beta. All the available chemicals were used without further purification.

### **Preparation of graphene suspension:**

Graphene suspension ( $0.05 \text{ mg mL}^{-1}$ ) was prepared by dispersing graphene nanosheets into dimethylformamide (DMF) solvent under sonication-assisted procedure. Typically, graphene-oxide (GO) was synthesized from natural graphite flakes by a modified Hummers method, and then GO was reduced through hydrothermal method at  $180 \text{ }^\circ\text{C}$  for 24 h to obtain graphene suspension. Next, graphene suspension was freeze dried and graphene nanosheets powder was achieved. After that, graphene powder (100 mg) was dispersed into DMF (200 mL), with sodium dodecyl benzene sulfonate (SDBS, 100 mg) added into graphene suspension as dispersant. High-power probe sonication was then carried out to make graphene nanosheets fully dispersed in the suspension.

### **Preparation of MHCF suspension:**

MHCF (M=Cu, Ni, Co, Fe) nanoparticle powders were synthesized by chemical co-precipitation. In a typical procedure, CuHCF nanoparticles were prepared by dropwise addition of copper chloride ( $\text{CuCl}_2$ ) aqueous solution (40 mM, 50mL) to potassium hexacyanoferrate ( $\text{K}_3\text{Fe}(\text{CN})_6$ ) aqueous solution (40 mM, 50 mL). The solution was stirred at 500 rpm and heated at  $70 \text{ }^\circ\text{C}$  for 8h. Then, the solution was washed through centrifugation at 5000 rpm for two times and dried at  $60 \text{ }^\circ\text{C}$ . After that, CuHCF powder was obtained. CuHCF suspension was further prepared via dispersing CuHCF powder (10 mg) into DMF (100 mL) with sonication assisted.

Similarly, NiHCF nanoparticles, CoHCF nanoparticles, and FeHCF nanoparticles were prepared by dropwise addition of nickel chloride ( $\text{NiCl}_2$ ) aqueous solution (40 mM, 50 mL), cobalt chloride ( $\text{CoCl}_2$ ) aqueous solution (40 mM, 50 mL), and ferric chloride ( $\text{FeCl}_3$ ) aqueous solution (40 mM, 50 mL) into potassium hexacyanoferrate ( $\text{K}_3\text{Fe}(\text{CN})_6$ ) aqueous solution (40 mM, 50 mL), respectively, following by the same procedures in the preparation of CuHCF suspension to obtain NiHCF suspension, CoHCF suspension, and FeHCF suspension.

**Fabrication of MHCF/graphene hybrid thin films with interdigital patterns:**

MHCF/graphene hybrid thin films (M=Cu, Ni, Co, Fe) were prepared through a mask-assisted filtration method. Typically, a lab-made mask with 10 interdigital-fingers (width of 1.6 mm, length of 15 mm, and interspace of 1.6 mm) was covered on the a polytetrafluoroethylene (PTFE) membrane filter (pore size of 0.2  $\mu\text{m}$ , diameter of 47 mm). Then, graphene suspension (2 mL) and MHCF suspension (2 mL) were alternately dropped on the mask and vacuum-filtrated, resulting in the formation of one layer graphene and one layer MHCF. By repeating such steps for ten times, MHCF/graphene composites with ten layers of graphene and ten layers of MHCF alternately stacked were obtained. Then, the resultant MHCF/graphene composites were directly transfer on the polyethylene terephthalate (PET) substrate to fabricate AMSCs with CuHCF/graphene served as one electrode and NiHCF/graphene, CoHCF/graphene, and FeHCF/graphene served as the other electrode, respectively.

**Materials characterization:**

Scanning Electron Microscopy (SEM) measurements and corresponding energy dispersive X-ray spectroscopy (EDX) elemental mapping were performed on field emission scanning electron microscope (FE-SEM) (Carl Zeiss Gemini 500). X-ray diffraction (XRD) patterns were measured on an X-ray diffractometer (D/max-2200/PC, Rigaku) using  $\text{Cu-K}\alpha$  radiation ( $\lambda = 1.5418 \text{ \AA}$ , voltage of 40 kV). Raman spectra were obtained using a Raman spectrometer (Renishaw inVia) with excitation laser wavelength of 532 nm at room temperature. Fourier transform infrared spectra (FTIR) were collected by Bruker Tensor 27 spectrometer. X-ray photoelectron

spectroscopy (XPS) measurements were conducted by AXIS Ultra DLD system from Kratos with Al K $\alpha$  radiation as X-ray source (1486.6 eV), anode voltage/current of 15 kV/10 mA.

**Electrochemical characterization:**

LiCl/PVA gel (2.12 g LiCl and 5 g PVA mixed with 50 ml deionized water), serving as electrolyte, was dropped on the MHCF/graphene films carefully and solidified overnight before electrochemical measurements. Besides, Cu foil was adhered on the end of microelectrode by silver paste as connector during electrochemical measurements. All the electrochemical measurements were conducted using CHI760D electrochemical work-station.

**Electrochemical calculations:**

The specific capacitance values of the device can be calculated from CV curves according to the following equation (1) and (2):

$$C_A = \frac{1}{2v \times A \times (V_f - V_i)} \int_{V_i}^{V_f} I(V) dV \quad (1)$$

$$C_V = \frac{1}{2v \times V \times (V_f - V_i)} \int_{V_i}^{V_f} I(V) dV \quad (2)$$

where  $C_A$  is donated as specific areal capacitance (mF cm<sup>-2</sup>) of MHCF/graphene-based AMSCs,  $v$  is the scan rate (V s<sup>-1</sup>),  $V_f$  and  $V_i$  are the integration voltage limits of the voltammetric curve, and  $I(V)$  is the voltammetric current with unit of ampere (A),  $A$  (cm<sup>2</sup>) is the area of the entire device.  $C_V$  is donated as specific volume capacitance (F cm<sup>-3</sup>) of MHCF/graphene-based AMSCs and  $V$  (cm<sup>3</sup>) is the volume of the entire device.

The specific areal capacitance ( $C_A$ , mF cm<sup>-2</sup>) and specific volume capacitance ( $C_V$ , F cm<sup>-3</sup>) of the entire AMSC on the basis of GCD curves can be obtained according to the following equation (3) and (4):

$$C_A = \frac{J \times \Delta t}{\Delta V} \quad (3)$$

$$C_V = \frac{C_A}{d} \quad (4)$$

where  $J$  is the current density ( $A m^{-2}$ ) of charge/discharge,  $\Delta t$  is the discharged time (s),  $\Delta V$  is voltage output window (V), and  $d$  is the thickness of MHCF/graphene-based AMSCs.

The volume energy density ( $E$ , Wh  $cm^{-3}$ ) and volume power density ( $P$ , W  $cm^{-3}$ ) of the entire device in the Ragone plot were calculated from GCD curves referred the equations (5) and (6) as follows:

$$E = \frac{1}{2} \times C_V \times \frac{(\Delta V)^2}{3600} \quad (5)$$

$$P = \frac{E}{\Delta t} \times 3600 \quad (6)$$

where  $C_V$  is specific volume capacitance of MHCF/graphene-based AMSCs,  $\Delta V$  is voltage output window (V), and  $\Delta t$  is the discharged time (s).

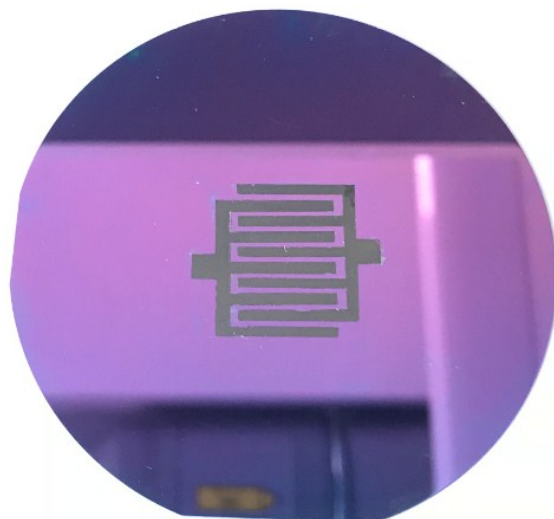


**Fig. S1** Photograph of Cu-Fe-AMSC transferred on the substrate of SiO<sub>2</sub>/Si wafer.

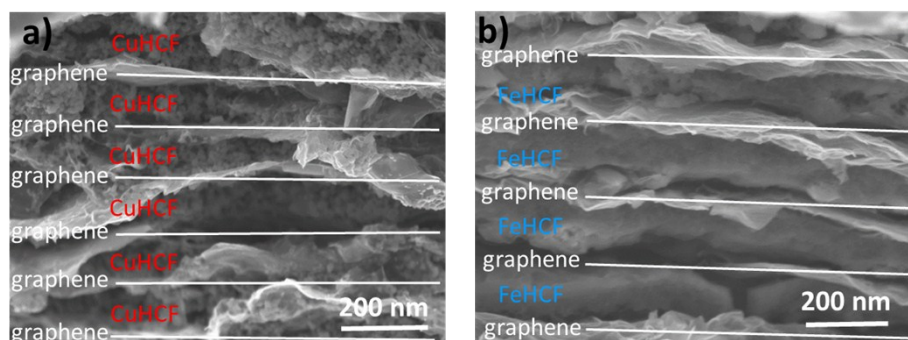


**Fig. S2** Cross-sectional SEM images of (a) CuHCF/graphene and (b) FeHCF/graphene hybrid thin films.

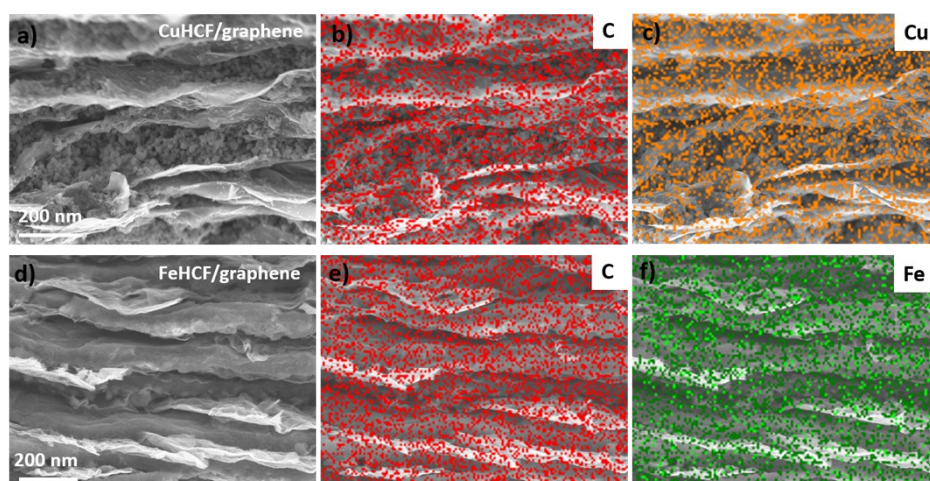


**Fig. S3** Cross-sectional SEM images and corresponding EDX elemental mapping of (a-c) CuHCF/graphene and (d-f) FeHCF/graphene.

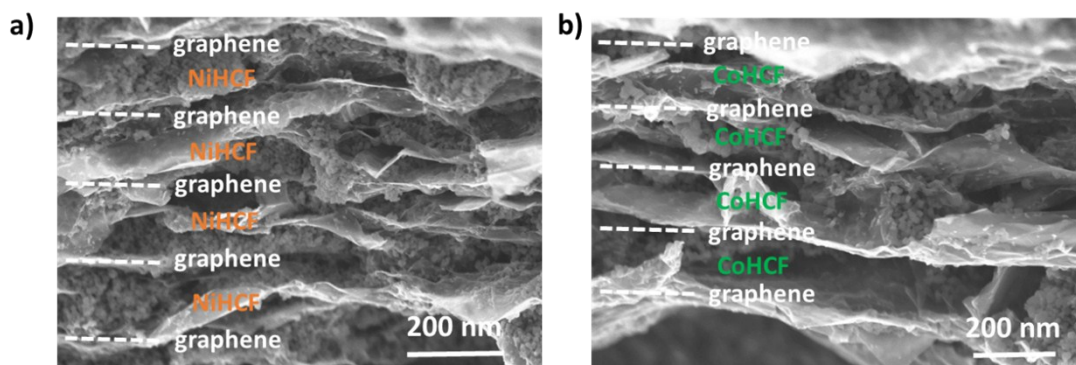


**Fig. S4** Cross-sectional SEM images of (a) NiHCF/graphene and (b) CoHCF/graphene hybrid thin films.

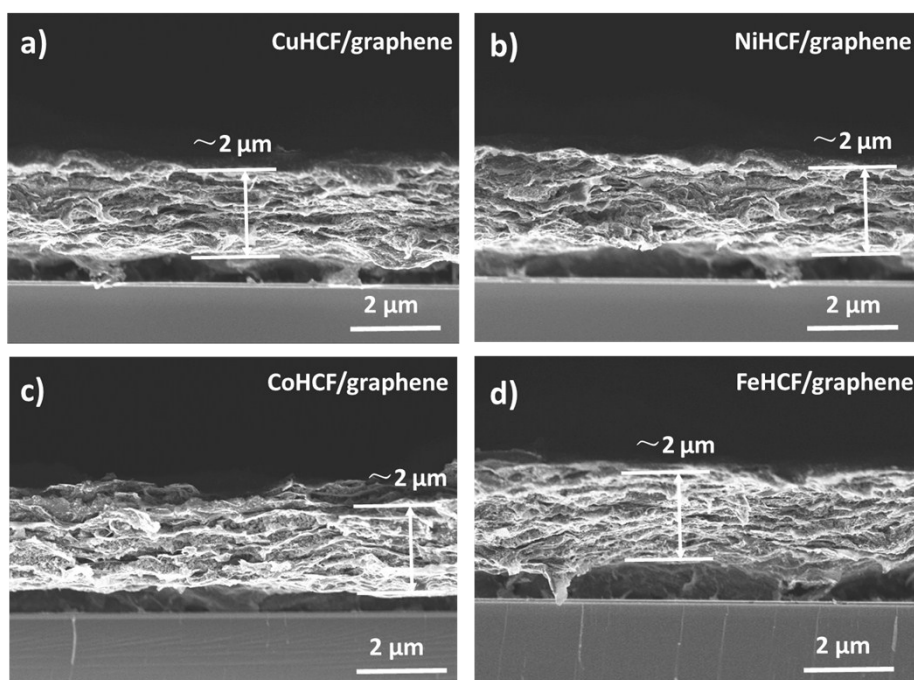


**Fig. S5** Overall cross-sectional SEM images of (a) CuHCF/graphene, (b) NiHCF/graphene, (c) CoHCF/graphene, and (d) FeHCF/graphene hybrid thin films.

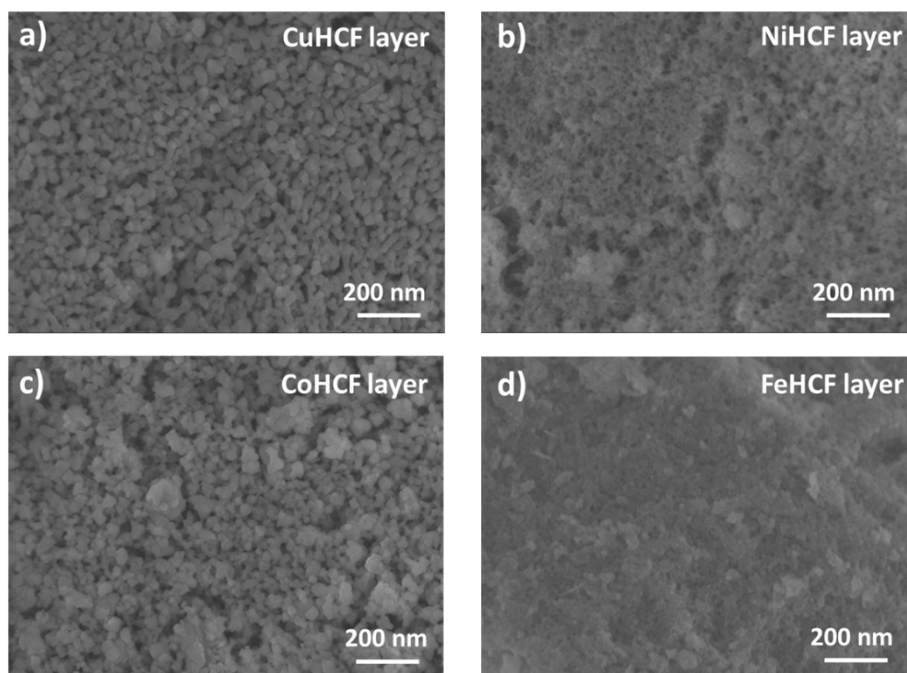


**Fig. S6** Top-view SEM images of (a) CuHCF layer for CuHCF/graphene films, (b) NiHCF layer for NiHCF/graphene films, (c) CoHCF layer for CoHCF/graphene films, and (d) FeHCF layer for FeHCF/graphene films.

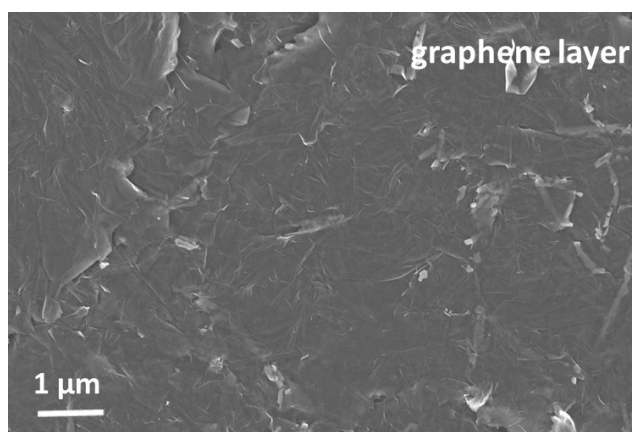


**Fig. S7** Top-view SEM image of graphene layer of CuHCF/graphene films.

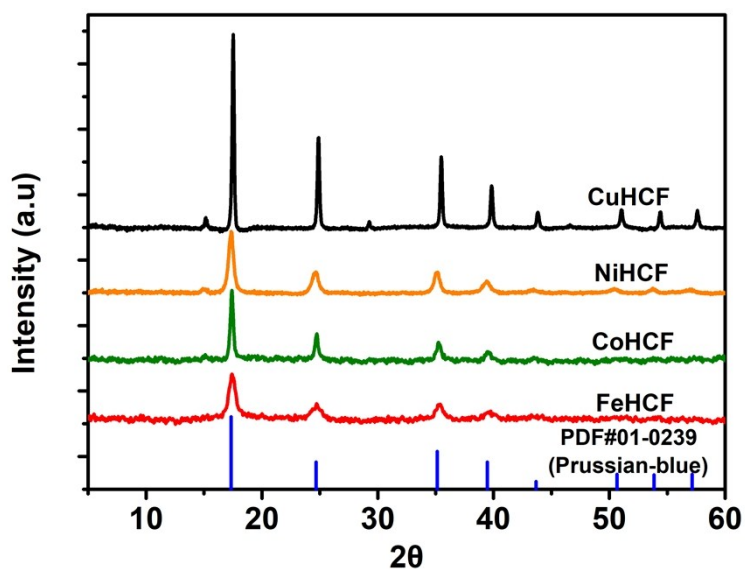


**Fig. S8** XRD patterns of as-prepared MHCF (M=Cu, Ni, Co, Fe) and standard face-centered-cubic Prussian blue crystal structure.

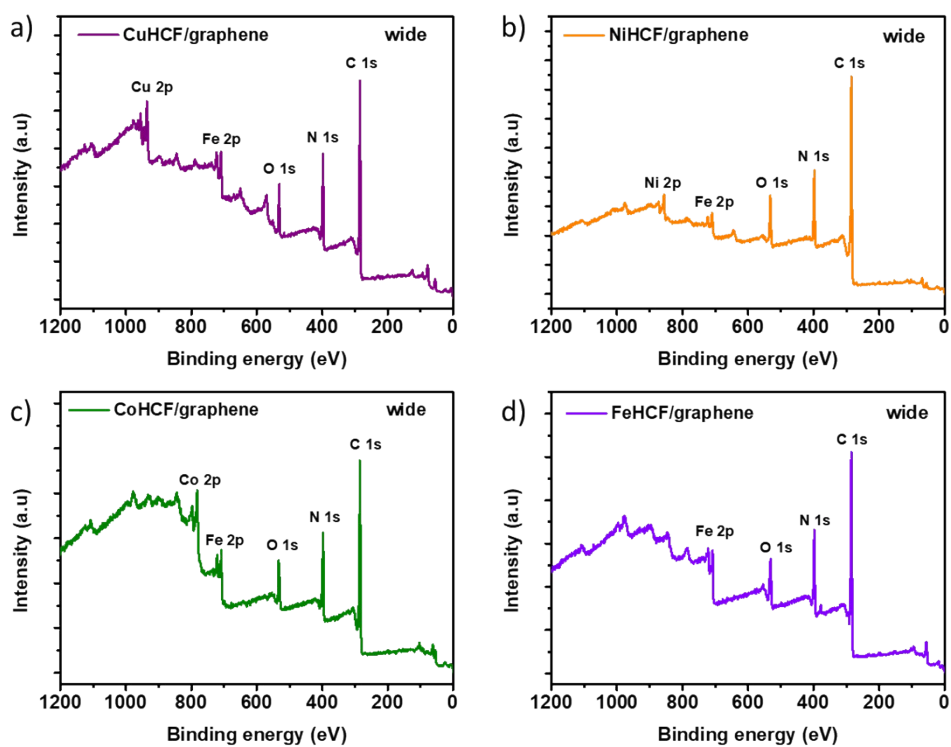


**Fig. S9** XPS wide spectra of (a) CuHCF/graphene, (b) NiHCF/graphene, (c) CoHCF/graphene, and (d) FeHCF/graphene.

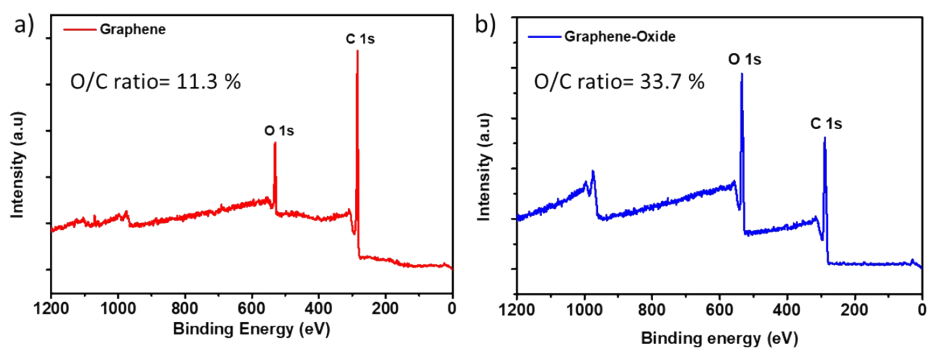


**Fig. S10** XPS survey spectra of (a) graphene and (b) original graphene-oxide with corresponding oxygen to carbon (C/O) atom ratios.

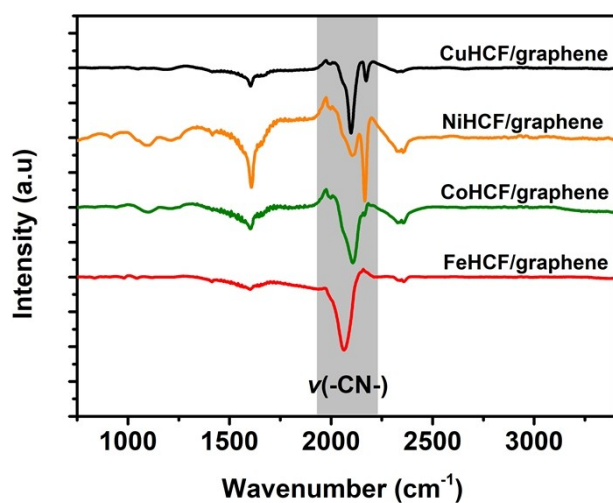


**Fig. S11** FTIR spectra of MHCF/graphene (M=Cu, Ni, Co, Fe) hybrid thin films.

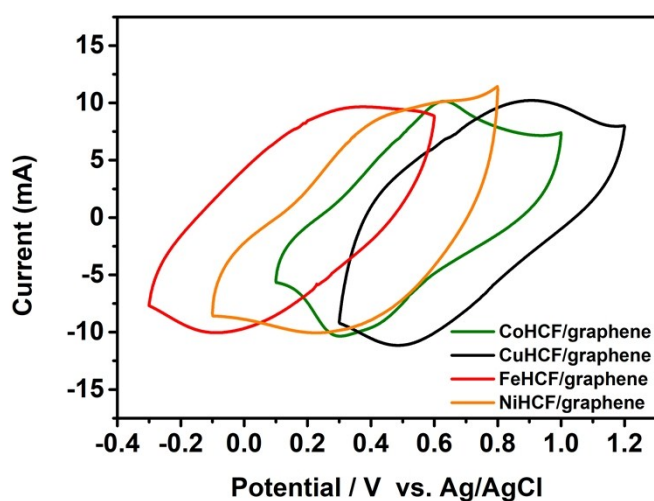


**Fig. S12** CV curves of MHCF/graphene (M=Cu, Ni, Co, Fe) hybrid thin films measured by standard three-electrode system.

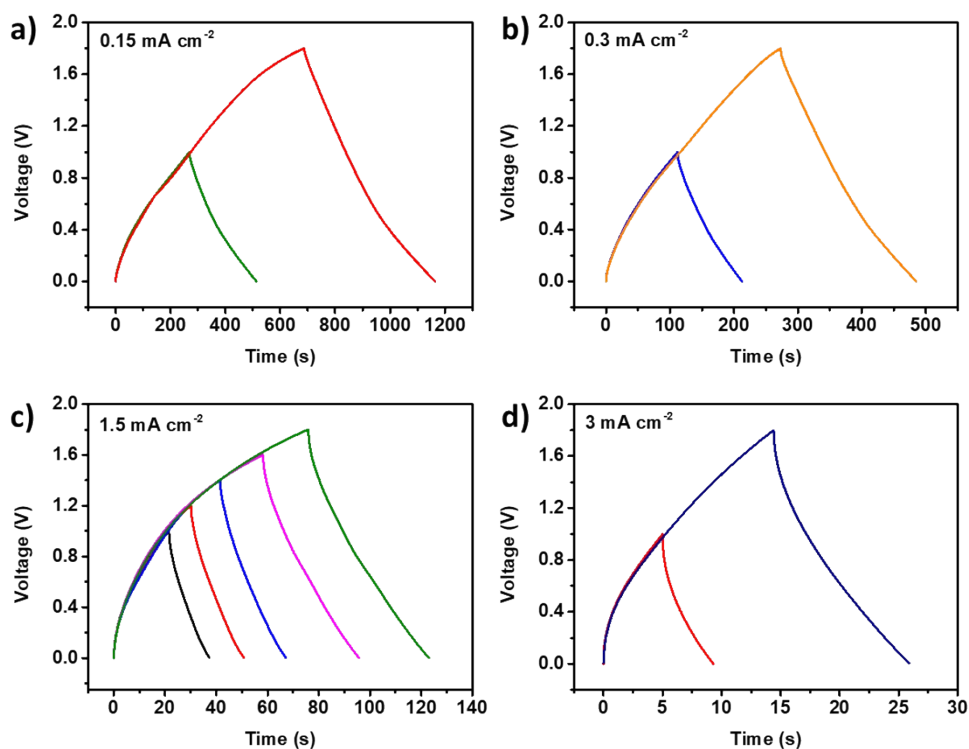


**Fig. S13** GCD curves of Cu-Fe-AMSC at current densities of (a)  $0.15 \text{ mA cm}^{-2}$ , (b)  $0.3 \text{ mA cm}^{-2}$ , (c)  $1.5 \text{ mA cm}^{-2}$ , and (d)  $3 \text{ mA cm}^{-2}$ .

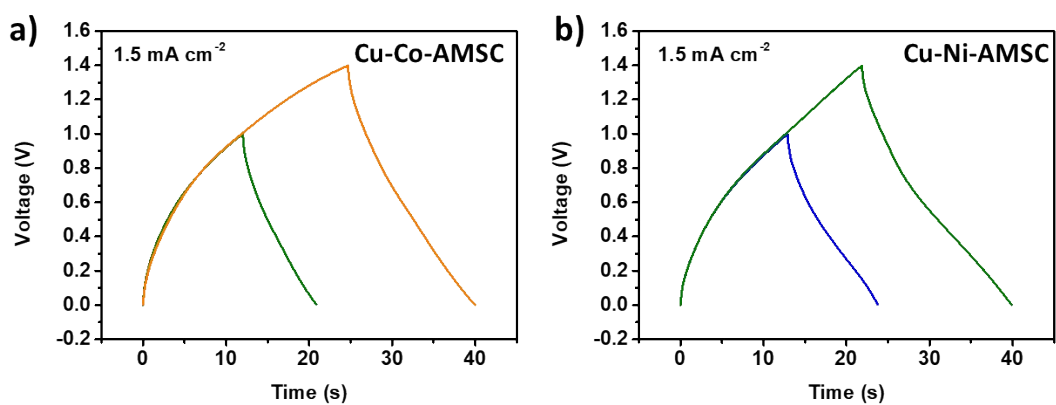


**Fig. S14** GCD curves of (a) Cu-Co-AMSC and (b) Cu-Ni-AMSC at a current density of  $1.5 \text{ mA cm}^{-2}$ .

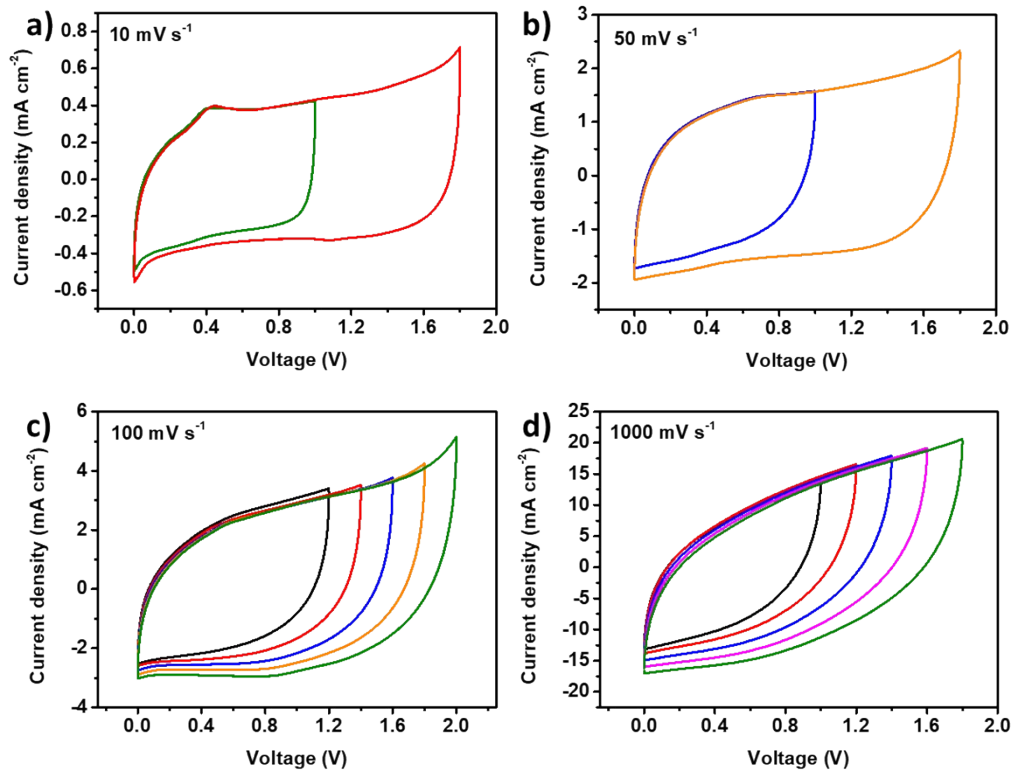


**Fig. S15** CV curves of Cu-Fe-AMSC at scan rates of (a) 10 mV s<sup>-1</sup>, (b) 50 mV s<sup>-1</sup>, (c) 100 mV s<sup>-1</sup>, and (d) 1000 mV s<sup>-1</sup>.

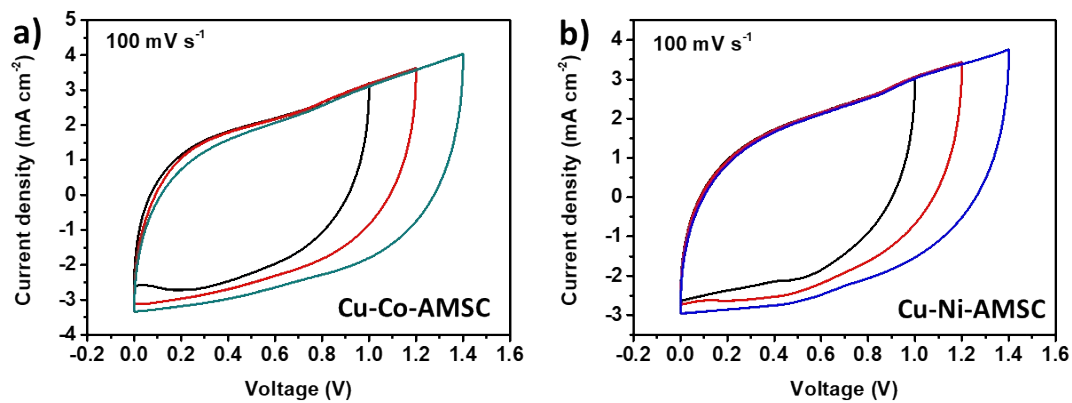


**Fig. S16** CV curves of (a) Cu-Co-AMSC and (b) Cu-Ni-AMSC at a scan rate of 100 mV s<sup>-1</sup>.

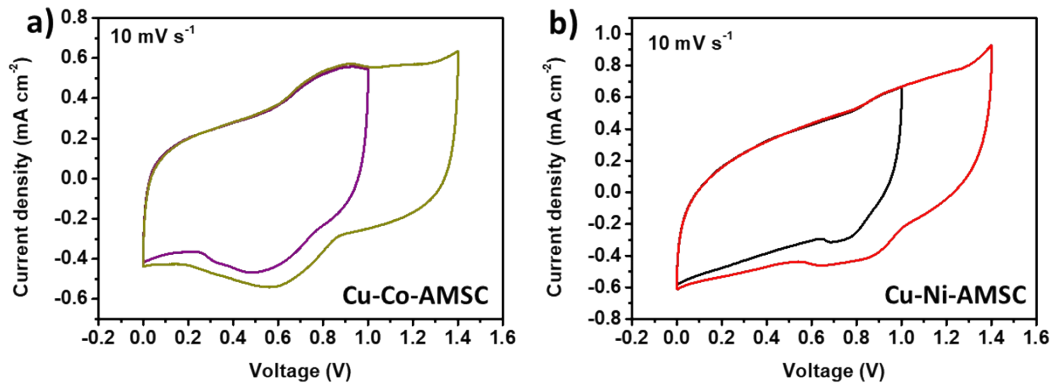


**Fig. S17** CV curves of (a) Cu-Co-AMSC and (b) Cu-Ni-AMSC at a scan rate of 10 mV s<sup>-1</sup>.

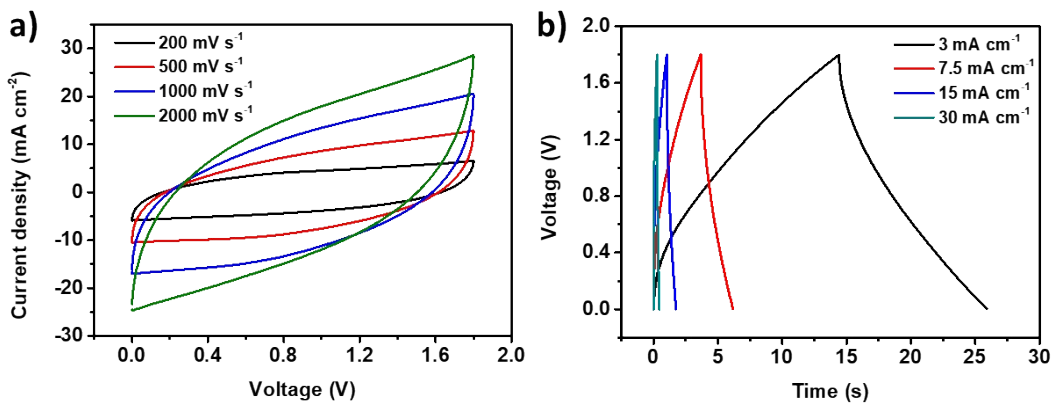


**Fig. S18** The capacitive behavior of Cu-Fe-AMSC under the voltage window of 1.8 V, including (a) CV curves at scan rates from 200 to 2000 mV s<sup>-1</sup> and (b) GCD curves at current densities from 3 to 30 mA cm<sup>-2</sup>.

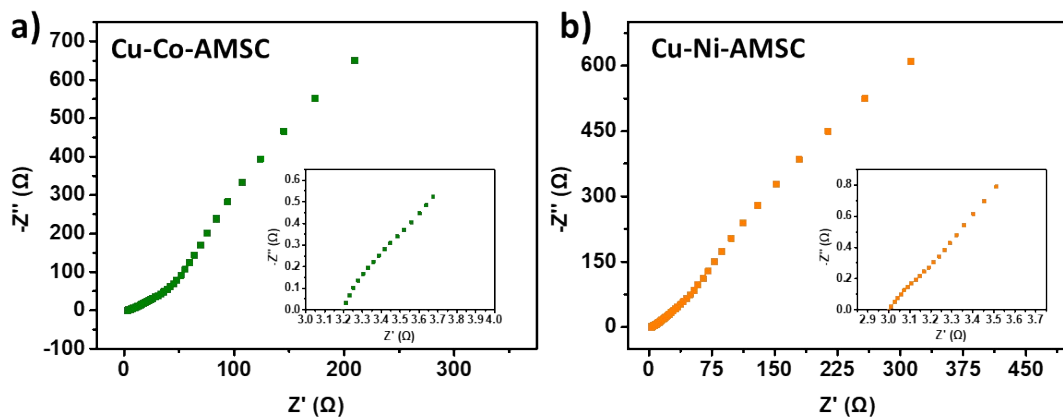


**Fig. S19** Nyquist plots of (a) Cu-Co-AMSC and (b) Cu-Ni-AMSC (inset shows the magnification of the high-frequency region).

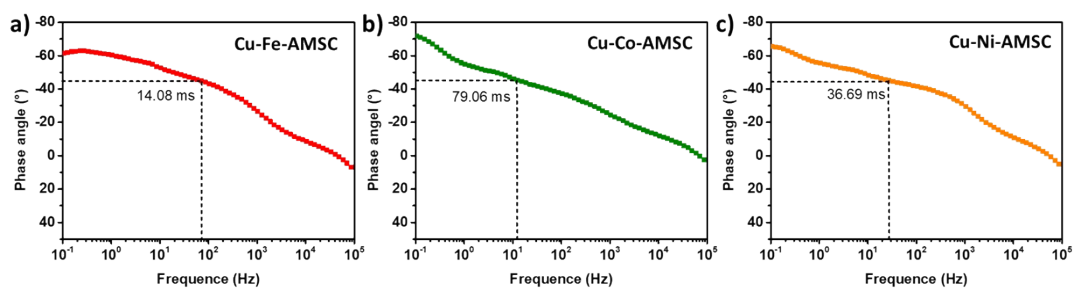


**Fig. S20** The impedance phase angle at different frequency and the corresponding RC time constant  $\tau_0$  for (a) Cu-Fe-AMSC, (b) Cu-Co-AMSC, and (c) Cu-Ni-AMSC.

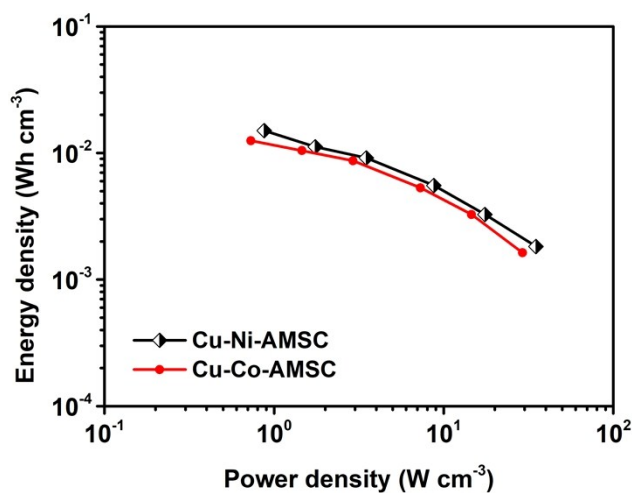


**Fig. S21** Ragone plots of Cu-Co-AMSC and Cu-Ni-AMSC.

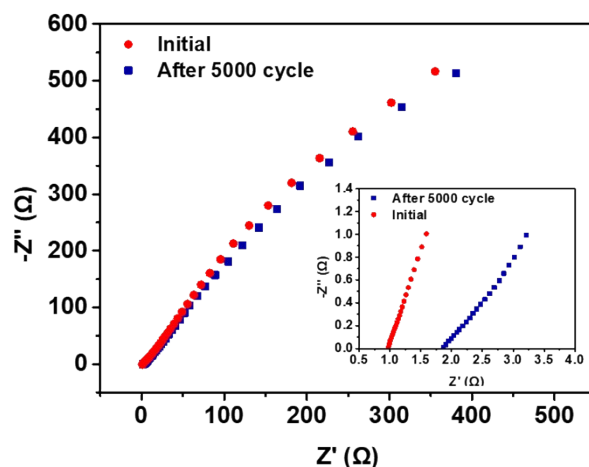


**Fig. S22** The Nyquist plots before and after 5000 charge/discharge cycles of Cu-Fe-AMSC (The inset shows the magnification of the high-frequency region of corresponding Nyquist plots).

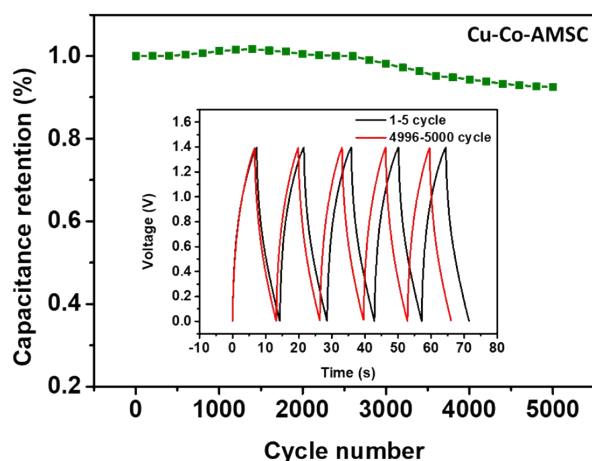


**Fig. S23** Cycling stability of Cu-Co-AMSC measured at  $3 \text{ mA cm}^{-2}$  under the voltage window of 1.4 V (inset shows the first five cycles and the last five cycles GCD curves).

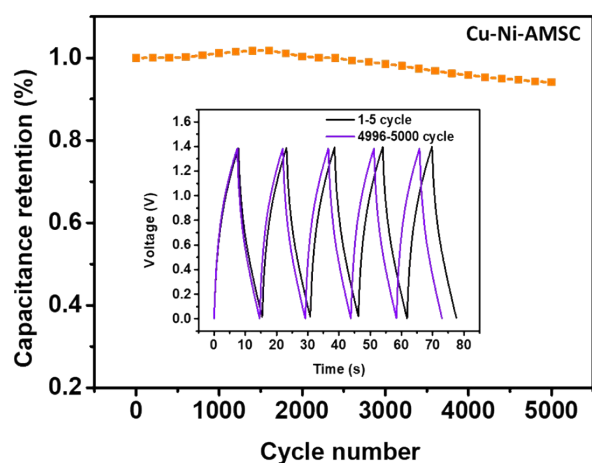


**Fig. S24** Cycling stability of Cu-Ni-AMSC measured at  $3 \text{ mA cm}^{-2}$  under the voltage window of 1.4 V (inset shows the first five cycles and the last five cycles GCD curves).

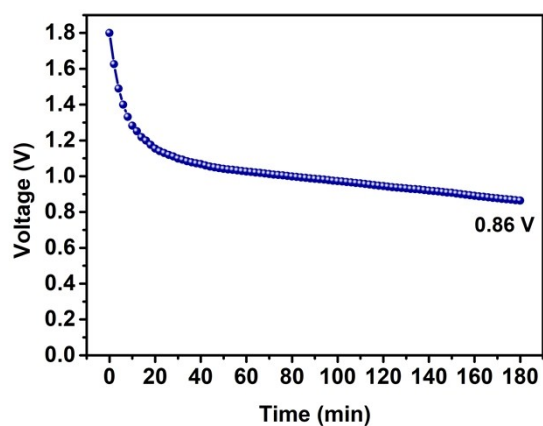


**Fig. S25** Self-discharge curve of Cu-Fe-AMSC.

**Table S1** The comparison of this work and previously reported MSCs.

Sample	Electrolyte	Areal capacitance (mF cm <sup>-2</sup> )	Energy density (mWh cm <sup>-3</sup> )	Type	Reference
Cu-Fe-AMSC	LiCl/PVA	19.8	44.6	Asymmetric	This work
Azulene-bridged coordination polymer framework	H <sub>2</sub> SO <sub>4</sub> /PVA	0.1	4.7	Symmetric	Angew. Chem. Int. Ed. 2017, 56, 3920
Thiophene nanosheets/graphene	H <sub>2</sub> SO <sub>4</sub> /PVA	3.9	13	Symmetric	Adv. Mater. 2017, 29, 1602960
Exfoliated graphene/V <sub>2</sub> O <sub>5</sub>	LiCl/PVA	3.92	20	Symmetric	Adv. Mater. 2017, 29, 1604491
MXene/graphene	H <sub>3</sub> PO <sub>4</sub> /PVA	3.26	3.4	Symmetric	Adv. Energy Mater. 2017, 7, 1601847
Phosphorene/graphene	Ionic liquid	9.8	11.6	Symmetric	ACS Nano 2017, 11, 7284
Laser-scribed graphene	H <sub>2</sub> SO <sub>4</sub> /PVA	2.32	0.4	Symmetric	Nat. Commun. 2013, 4, 1475
PANI nanowires	H <sub>2</sub> SO <sub>4</sub> /PVA	45.2	0.8	Symmetric	Adv. Energy Mater. 2014, 4, 1301269
TiO <sub>2</sub> /reduced graphene-oxide	H <sub>2</sub> SO <sub>4</sub> /PVA	1.5	7.7	Symmetric	ACS Nano 2017, 11, 4283
d-Ti <sub>3</sub> C <sub>2</sub> //AC	K <sub>2</sub> SO <sub>4</sub> solution	-	1.0	Asymmetric	Science 2013, 341, 1502
graphene-FeOOH//graphene-MnO <sub>2</sub>	H <sub>2</sub> SO <sub>4</sub> /PVA	934	2.4	Asymmetric	Adv. Mater. 2016, 28, 838
K <sub>2</sub> Co <sub>3</sub> (P <sub>2</sub> O <sub>7</sub> ) <sub>2</sub> //graphene	KOH/PVA	1100	0.96	Asymmetric	Nano Energy 2015, 15, 303

**Table S2** The comparison of this work and previously reported asymmetric supercapacitors.

Sample	Electrolyte	Cycling stability	Reference
<b>Cu-Fe-AMSC</b>	<b>LiCl/PVA</b>	<b>96.8% after 5000 cycles</b>	<b>This work</b>
H-TiO <sub>2</sub> @MnO <sub>2</sub> //H-TiO <sub>2</sub> @C	LiCl/PVA	91.2% after 5000 cycles	Adv. Mater. 2013, 25, 267
MnO <sub>2</sub> NW/graphene//graphene	Na <sub>2</sub> SO <sub>4</sub> solution	79% after 1000 cycles	ACS Nano 2010, 4, 5835
MnO <sub>2</sub> //graphene hydrogel	Na <sub>2</sub> SO <sub>4</sub> solution	83.4% after 5000 cycles	ACS Appl. Mater. Interfaces 2012, 4, 2801
RuO <sub>2</sub> /graphene//graphene	H <sub>2</sub> SO <sub>4</sub> /PVA	95% after 2000 cycles	Nanoscale 2012, 4, 4983
MnO <sub>2</sub> //PPy	LiCl/PVA	~80% after 5000 cycles	J. Mater. Chem. A 2016, 4, 9502
VN//Co(OH) <sub>2</sub> -PHMSs	KOH/PVA	~88% after 5000 cycles	npj 2D Materials and Applications 2018, 2, 7
graphene-FeOOH//graphene-MnO <sub>2</sub>	H <sub>2</sub> SO <sub>4</sub> /PVA	84% after 2000 cycles	Adv. Mater. 2016, 28, 838
K <sub>2</sub> CO <sub>3</sub> (P <sub>2</sub> O <sub>7</sub> ) <sub>2</sub> //graphene	KOH/PVA	94.4% after 5000 cycles	Nano Energy 2015, 15, 303
graphene quantum dots//MnO <sub>2</sub>	Ionogels	80% after 3000 cycles	ACS Appl. Mater. Interfaces 2015, 7, 25378
VN//Co(OH) <sub>2</sub>	KOH solution	86% after 4000 cycles	J. Mater. Chem. A 2014, 2, 12724